Neutron Stars and Gravitational Waves

Author: Patrícia Gimeno Estivill
Facultat de Física, Universitat de Barcelona, Martí i Franquès 1, 08028 Barcelona, Spain.

Advisor: Àngels Ramos Gomez

Abstract: On the basis of a simple model for the energy of nuclear matter, we parametrize different equations of state within the constraints of experimental data to describe neutron stars with masses larger than 2M$_\odot$. Furthermore, we predict the dimensionless tidal deformability for a family of neutron stars characterized by the mass-radius relation computed from each equation of state. The obtained results are compared with recent observations of millisecond pulsars and gravitational-wave data to conclude with the choice of the best parametrized equation of state to describe the neutron stars observed.

I. INTRODUCTION

The formation of a neutron star results from the gravitational-collapse of a massive star in its last evolutionary stage. In this process, the massive star's core is compressed to a very high density and the β-decay reaction is triggered - the vast majority of protons and electrons are transformed into neutrons and anti-neutrinos. Then, the high degeneracy pressure of these new neutrons halts the initial collapse and all the material surrounding the core is ejected producing a supernova explosion. The resulting compact object made up of neutrons and a fewer number of protons, electrons and other particles is known as a Neutron Star(NS), detectable on Earth by its emission of photons, neutrinos or gravitational waves from a binary neutron star merger.

The fundamental properties of a NS are obtained from the Equation of State (EoS) which determines the relationship between pressure and energy density in nuclear matter. However, it is difficult to definitively describe and experimentally reproduce the composition of the core because of the supra-nuclear density matter.

In this project, we describe the nuclear matter layer of a NS using different parametrized EoS which are calibrated by experimental constraints imposed by data from heavy-ion collisions (HIC) in symmetric nuclear matter and extrapolated to pure neutron matter. With the parameters selected we compute new EoS in β-stable matter to calculate the mass M, radius R and dimensionless tidal deformability Λ of a collection of NS to make a comparison with observed millisecond pulsars stars [1, 2] as well as with the recent observations by NICER (Neutron Star Interior Composition ExploreR)[3, 4] and by the Advanced LIGO and VIRGO detectors from the GW170817 event[5, 6]. The objective is to model an EoS based on the best parameter values to describe the recent NS observations.

II. THE EQUATION OF STATE

A. Parametrization of nuclear matter at T=0

In order to calculate a non-relativistic EoS at zero temperature, we use the simple parametrization of the nucleonic energy per baryon of Heiselberg and Hjorth-Jensen[7]

$$\epsilon(n, x_p) = \epsilon_0 u \frac{u - 2 - \delta}{1 + u\delta} + s_0 u^\gamma (1 - 2x_p)^2 \tag{1}$$

where $u = n/n_0$ is the baryon density assuming only protons and neutrons ($n = n_p + n_n$) measured with respect to the nuclear saturation density, n_0=0.16 fm^{-3}, and $x_p = n_p/n$ is the proton fraction.
We can redefine Eq. (1) by expanding the energy density about the value for the symmetric case $x_p = 1/2$ to distinguish a compressional term and a symmetry term:

$$\begin{aligned}\epsilon(n, x_p) &= \epsilon(n, x_p = \frac{1}{2}) + \frac{1}{2}\left(\frac{d^2\epsilon}{d^2x}(n)\right)(x_p - \frac{1}{2})^2 + ...\\ &\simeq \epsilon(n, x_p = \frac{1}{2}) + 4\mathcal{S}(n)(x_p - \frac{1}{2})^2\\ &= \mathcal{E}_{comp}(n) + \mathcal{S}(n)(1 - 2x_p)^2\end{aligned} \tag{2}$$

In Eq. (2) we can relate the quadratic term coefficient of the expansion to the so-called symmetry energy $\mathcal{S}(n)$. This term reflects the variation of the binding energy of nucleons between pure neutron matter (PNM) and symmetric nuclear matter (SNM), that is, $\mathcal{S}(n) = \epsilon(n, x_p = 0) - \epsilon(n, x_p = 1/2) = s_0 u\gamma$. For this model, Heiselberg *et al.* established the symmetry energy coefficient and the binding energy per nucleon at the saturation density, resulting in s_0 = 32MeV and $\epsilon_0 = -15.8$ MeV, respectively. In the same way, the slope parameter, defined as $L = 3n_0\left(\frac{\partial S(n)}{\partial n}\right)_{n_0} = 3s_0\gamma$ at the saturation density, was taken to be 57 MeV, which determined the value of the parameter $\gamma = 0.6$. On the other hand, the parameter $\delta = 0.2$ was assigned so that the EoS does not violate the Causality Principle[7].
Finally, the system pressure is obtained through the equation $P = n\frac{\partial\epsilon}{\partial n} - \epsilon$ with dimensions of MeV·fm^{-3}.

B. Constraints on the Equation of State

1. Heavy-ion collision data

On the basis of a set of initial densities, we implemented Eq. (1) in Fortran to obtain a collection of four parametrized EoS classified by the parameters γ and δ. For the former, we applied its original value of $\gamma = 0.6$, as well as $\gamma = 0.4$, since this value reproduces a slope parameter consistent with new theoretical constraints developed by Oertel *et al.*[8] and Roca-Maza *et al.*[9]. We chose the parameter δ according to experimental constraints imposed by data from heavy-ion collisions (HIC) at high energy. In these experiments, the nuclear matter is compressed to densities that can be achieved within NS and in supernovae explosions [10]. Thus, we restrained our computed EoS to lie within the shaded region defined by this data, as it is seen in Fig. 1. Finally, we selected the minimum value of $\delta = 0.05$ to study the EoS located at the edge of this area, as well as the EoS with $\delta = 0.2$, the original parameter of the model.

III. NEUTRON STAR PROPERTIES

A. β-stable neutron star matter

Although we have worked on SNM and PNM to calibrate the parametrized EoS, the description of neutron stars requires the EoS of β-stable matter. In this model, NS are mainly composed of neutrons but also of a small number of protons and electrons in chemical equilibrium. Before a NS is formed, the particles within the core of the original massive star are compressed to such densities that they reach the highest energy (Fermi level) due to the Pauli exclusion principle. As a result, the weak β-decay process $n \to p + e^- + \bar{\nu}_e$ is halted in the NS because of the presence of these protons and neutrons at the highest Fermi level.
In this regime, the decay reaction is balanced with the electron capture:

$$n \to p + e^- + \bar{\nu}_e \qquad\qquad p + e^- \to n + \nu_e \tag{3}$$

This balance is imposed by the following relation between chemical potentials:

$$\mu_n = \mu_p + \mu_{e^-} \tag{4}$$

where the neutrinos do not appear in the balance because they freely escape from the star.
In addition, the baryon number $n = n_p + n_n$ is conserved and the charge neutrality is ensured by imposing $k_{Fp} = k_{Fe}$, also expressed as $n_p = n_e$.
Finally, we can determine the general relation in Eq. (5) by assuming relativistic electrons and applying the simple formula $\mu_i = \partial E/\partial N_i$ where $i = p, n$.

$$\begin{aligned} \mu_e &= \mu_n - \mu_p \\ &= 4s(n)(1 - 2x_p) \\ &= \hbar c(3\pi^2 n x_p)^{1/3} \end{aligned} \tag{5}$$

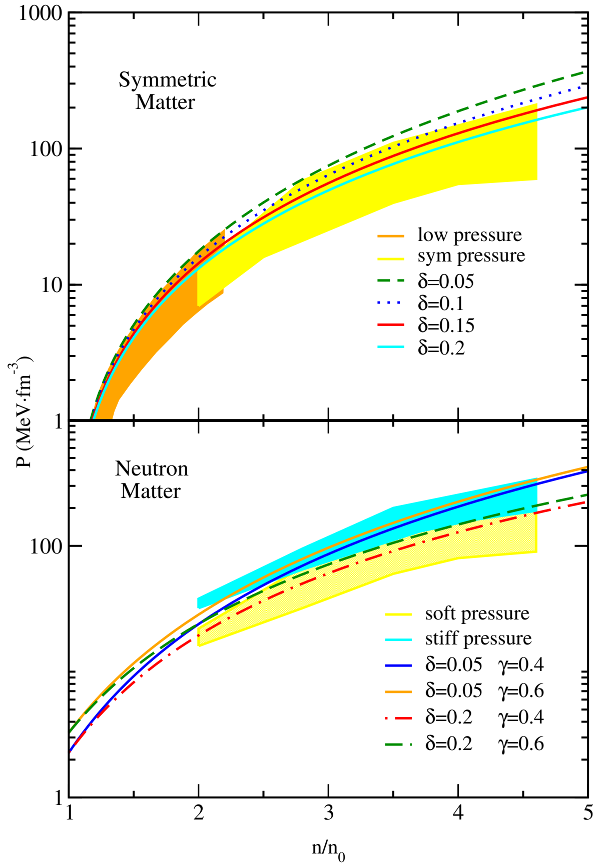

Figure 1: Comparison of the pressure values as a function of the baryon density between the four EoS and the experimental data from HIC (shaded regions). In the upper panel, the EoS are computed for SNM and compared with the regions compatible with collective flow [10](yellow) and kaon production data [11, 12](orange). In the lower panel we depict the EoS for PNM including the pressure obtained from HIC data adding a soft(yellow) and a stiff(blue) symmetry energy [10]. It is remarkable that in SNM, the lower the parameter δ, the stiffer the EOS at any density while in PNM a lower value of γ softens the EoS, especially at low densities.

For this model, we also took into account the presence of muons $\mu_e = \mu_\mu = \sqrt{m_\mu^2 + k_{F\mu}^2}$ in charge balance with protons and electrons $n_e + n_\mu = n_p$. Thus, Eq. (5) can be rewritten as:

$$[4s(n)(1-x_p)]^3 + \{[4s(n)(1-2x_p)]^2 - m_\mu^2\} = 3\pi^2 n x_p \tag{6}$$

With these equations we can correctly determine x_p for each given $u = n/n_0$ and therefore the composition of β-stable neutron matter.

B. TOV equations: Mass and Radius of Neutron Stars

The mass M and the radius R of a non-rotating NS are obtained by solving the Tolman-Oppenheimer-

Volkoff(TOV) equations for hydrostatic equilibrium:

$$\begin{aligned}\frac{dM(r)}{dr} &= 4\pi e(r)r^2\\ \frac{dp(r)}{dr} &= -\frac{[p(r)+e(r)][M(r)+4\pi r^3 p(r)]}{r(r-2M(r))}\end{aligned} \tag{7}$$

Imposing the boundary conditions $M(r=0)=0$ and $P(r=R)=0$ and assuming different values of central energy density $\epsilon(r=0)=\epsilon_c$ we obtained the mass-radius relation shown in Fig. 2 from the four parametric EoS in β-stable matter. The two EoS having $\delta=0.05$ can describe NS greater than the most massive ever observed, PSR J0740+6620[2], as well as the PSR J0348+0432[1].

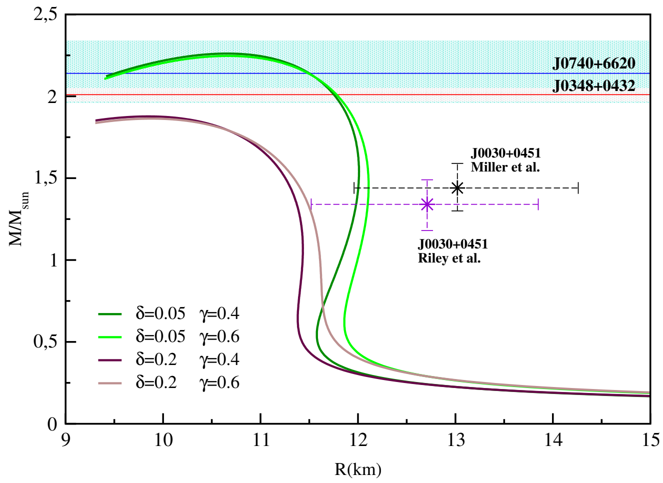

Figure 2: The solid lines indicate the mass-radius relationship of NS from the four parameterized EoS. The horizontal lines represent some high-mass observational values: PSR J0740+6620[2] of M=$2.14^{+0.20}_{-0.18}M_\odot$(blue) and J0348+0432[1] of M=$2.01^{+0.04}_{-0.04}M_\odot$(red). The recent observation of J0030+0451 by NICER is shown as a magenta star with M=$1.34^{+0.15}_{-0.16}M_\odot$ and R=$12.71^{+1.14}_{-1.19}$ Km in the analysis done by Riley *et al.*[4] and as a black star with M=$1.44^{+0.15}_{-0.14}M_\odot$ and R=$13.01^{+1.24}_{-1.06}$ Km in the model by Miller *et al.*[3].

In contrast, the EoS parametrized with $\delta=0.2$ describe NS with lower masses than these observations, as can be seen in Fig. 2.

Comparing with the recent observation of PSR J0030+045 by the X-Ray Telescope NICER, which provides a simultaneous measurement of the mass M and the radius R of the star, we see that the obtained mass-radius curves with $\delta=0.05$ are compatible with this observation. However, the two EoS with $\delta=0.2$ predict the values of the radius outside of the margin of error of both analyses.

The significant masses and radii computed from each parametrized EoS are shown on the left-hand-side of Table I, which allows to easily compare them with results on the righ-hand side obtained from different observations.

C. Tidal deformability

When two NS merge in a binary system and the distance between them becomes comparable to their radii, the tidal forces on each other begin to deform them. This produces a quadrupole moment, Q_{xy}, related to the external field through the tidal deformability λ[5, 13]:

$$Q_{xy} = \lambda E_{xy} \qquad E_{xy} = -\frac{\partial V_G}{\partial x \partial y} \tag{8}$$

This quadrupole deformation affects the binding energy of the system and there is an increase in the rate of emission of gravitational waves[14]. Thus, the recent detection of the gravitational wave signal GW170818 by LIGO and VIRGO detectors[5] is a consequence of the tidal properties of the NS, commonly expressed as:

$$\lambda = \frac{2}{3}k_2 R^5 \tag{9}$$

where k_2 is the gravitational Love number calculated from[13]:

$$\begin{aligned}k_2 = &\frac{8C^5}{5}(1-2C)^2[2+2C(y_R-1)-y_R]\times\\ &\{2C[6-3y_R+3C(5y_R-8)]+\\ &4C^3[13-11y_R+C(3y_R-2)+2C^2(1+y_R]+\\ &3(1-2C)^2[2-y_R+2C(r_R-1)]ln(1-2C)\}^{-1}\end{aligned} \tag{10}$$

and $C=M/R$ is the compactness parameter. The value for $y_R \equiv y(R)$ is obtained by solving the following differential equation together with the TOV Eqs. (7) and the boundary condition $y(0)=2$:

$$\begin{aligned}&ry'(r)+y(r)^2+\\ &y(r)e^{\lambda(r)}[1+4\pi r^2(p(r)-\epsilon(r))]+r^2Q(r)=0,\end{aligned} \tag{11}$$

where $e^{\lambda(r)}=(1-\frac{2M(r)}{r})^{-1}$ is a metric function of a spherical star and

$$\begin{aligned}Q(r) = &4\pi e^{\lambda(r)}\left(5e(r)+9p(r)+\frac{\epsilon(r)+p(r)}{c_s^2}\right)\\ &-6e^{\lambda(r)}r^{-2}-(\nu'(r))^2,\end{aligned} \tag{12}$$

with $\nu'(r)^2$ the derivative of the $\nu(r)$ metric function:

$$\nu'(r) = 2e^{\lambda(r)}\frac{M(r)+4\pi p(r)r^3}{r^2} \tag{13}$$

and $c_s^2 = dp/de$ the square of the speed of sound.

Because the tidal deformability contains information on the internal structure of the NS, the radius of the individual components of binary NS systems can be estimated through gravitational wave data. Furthermore, from the observations by NICER, new methods have been derived to measure this property, which is very difficult to accurately estimate from other sources[15].

	$\delta = 0.05$, $\gamma = 0.4$	$\delta = 0.05$, $\gamma = 0.6$	$\delta = 0.2$, $\gamma = 0.4$	$\delta = 0.2$, $\gamma = 0.6$
$\boldsymbol{M_{max}(M_\odot)}$	2.26	2.25	1.88	1.86
$\boldsymbol{R_{M_{max}}(Km)}$	10.66	10.67	9.85	9.88
$\boldsymbol{\tilde{\Lambda}_{M_{max}}}$	320.43	357.67	276.68	300.98
$\boldsymbol{R_{1.4M_\odot}(Km)}$	12.00	12.12	11.34	11.44
$\boldsymbol{\Lambda_{1.4M_\odot}}$	364.35	395.79	240.37	253.725
$\boldsymbol{\tilde{\Lambda}}$	440.56	471.61	294.70	312.22

J0348+0432	**J0740+6620**	**J0030+0451** Riley *et al.*	**J0030+0451** Miller *et al.*	**GW 170817** NS_1	**GW 170817** NS_2	
$2.01^{+0.04}_{-0.04}$	$2.14^{+0.20}_{-0.18}$	$1.34^{+0.15}_{-0.16}$	$1.44^{+0.15}_{-0.14}$	(1.36-1.60)	(1.17-1.36)	$\boldsymbol{M(M_\odot)}$
		$12.71^{+1.14}_{-1.19}$	$13.01^{+1.24}_{-1.06}$	$10.8^{+2.0}_{-1.7}$	$10.7^{+2.1}_{-1.5}$	$\boldsymbol{R(Km)}$
				800≥		$\boldsymbol{\Lambda_{1.4M_\odot}}$
				800≥		$\boldsymbol{\tilde{\Lambda}}$

TABLE I: The left-hand-side table shows for each parametrization the mass M, radius R and dimensionless tidal deformability Λ of the most massive NS as well as the R and Λ for a NS with $1.4M_\odot$. The last row shows the combined dimensionless tidal deformability $\tilde{\Lambda}$. In the right-hand-side table we present the mass results for the observed NS J0348+0432[1], J0740+6620[2] and also the masses and radii for J0030+045[3, 4]. The last column specifies the estimated masses of the binary neutron system assuming the dimensionless spin $|\chi| \leq 0.05$ from the GW170817 event, as well as their radii and the constraints $\Lambda_{1.4M_\odot} \leq 800$ and $\tilde{\Lambda} \leq 800$ obtained from this detection[5, 6]

A related quantity is the dimensionless tidal deformability Λ:

$$\Lambda \equiv \frac{\lambda}{m^5} = \frac{2}{3}k_2\frac{R^5}{m^5} = \frac{2}{3}\frac{k_2}{C^5} \tag{14}$$

In Fig. 3 it can be seen that the value for Λ fits better with the inverse sixth power rather than the fifth power of mass as defined in Eq. (14). As Chatziioannou explains in [14], the additional factor of m is a consequence of the tidal Love number k_2, which is inversely proportional to it.

It is also noteworthy that for a given EoS, Λ varies from roughly 10^3 in $1M_\odot$ stars to a little over 10 for $M > 2M_\odot$, the most massive stars. Furthermore, at a fixed mass in the range of $M > 1.3M_\odot$, different EoS predict different values of Λ with a difference of more than one order of magnitude. In conclusion, less massive NS are less compact with a large value of Λ since they are more easily deformable than massive NS, further explained in [14]. On the other hand, if we study a binary system we can compute a new parameter $\tilde{\Lambda}$ and the chirp mass $\mathcal{M}$ via the dimensionless tidal deformability of each component, $\Lambda_1(M_1)$ and $\Lambda_2(M_2)$ with $M_1 > M_2$, as:

$$\tilde{\Lambda} = \frac{16}{13}\frac{(M_1 + 12M_2)M_1^4\Lambda_1 + (M_2 + 12M_1)M_2^4\Lambda_2}{(M_1 + M_2)^5} \tag{15}$$

$$\mathcal{M} = \frac{(M_1 M_2)^{3/5}}{(M_1 + M_2)^{3/5}} \tag{16}$$

On the basis of the constrained values of $\mathcal{M} = 1.188^{+0.004}_{-0.002}M_\odot$ and $M_1 \subset (1.36, 1.69)$, $M_2 \subset (1.17, 1.36)$ by the LIGO-Virgo collaboration in [5], we assigned the mass results $M \geq 0.5$ obtained in Fig. 2 as the mass M_1, the larger component of different binary stars. For each M_1, we calculated the mass companion M_2 from Eq. (16). The corresponding Λ_1 and Λ_2 values, derived from the $\Lambda(M)$ relationship shown in Fig. 3, are represented, one versus the other, in Fig. 4.

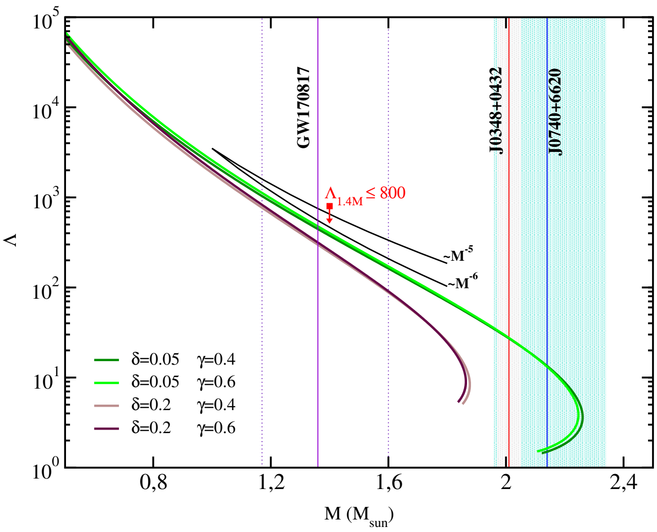

Figure 3: Dimensionless tidal deformability Λ as a function of the NS mass $M(M_\odot)$ from the four models of EoS. The black lines indicate the trend proportional to M^{-5} and M^{-6} while the purple vertical lines represent the predicted mass-ranges (1.17-1.36)$M_\odot$ and (1.36-1.60)$M_\odot$ from GW170817[5] assuming the dimensionless spin $|\chi| < 0.05$. The red square with the downward arrow denotes the $\Lambda_{1.4M} \leq 800$ constraint[5]. In addition, we plotted the mass results of J0348+0432[1] and J0740+6620[2] in red and blue vertical lines, respectively.

IV. CONCLUSIONS

In this project we computed different parametrized EoS in β-equilibrium matter to describe NS and study their concordance with recent observations. Based on the model of the nucleonic energy per baryon of Heiselberg and Hjorth-Jensen[7], we selected the original parameters $\delta = 0.2$ and $\gamma = 0.6$ of the model and also $\delta = 0.05$ and $\gamma = 0.4$ within the constraints imposed by data from heavy-ion collisions (Fig. 1) and by the slope parameter $L = 3s_0\gamma = 57$ MeV measured at the

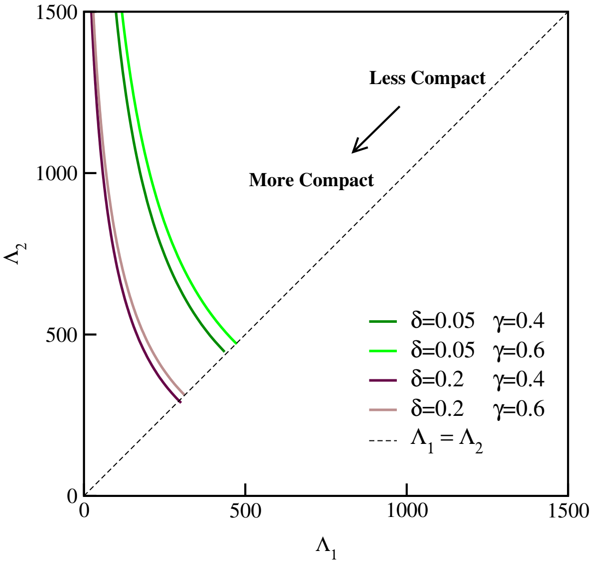

Figure 4: Estimated values of Λ_1 and Λ_2 located at the 50% of the probability region predicted from GW170817 [5], corresponding to the high (M_1) and low (M_2) mass components of binary neutron star systems.

saturation density, $n_0 = 0.16$ fm^{-3}. Finally, we calculated the mass-radius relation from each parametrized EoS, shown in Fig. 2, as well as the dimensionless tidal deformability, Fig. 3 and 4, and the combined dimensionless tidal deformability of different binary neutron star systems.

From the results in Table I, we can notice that:

- with $\delta = 0.05$ we predict maximum neutron star masses that are compatible to the mass of $2.14^{+0.20}_{-0.18} M_{\odot}$, the highest mass observed so far[2].
- the mass-radius relations computed from the EoS with $\delta = 0.05$ are compatible with the simultaneous measurements of the mass and the radius of PSR J0030+45, detected by NICER[3, 4].
- with the model studied, the dimensionless tidal deformability and the combined dimensionless tidal deformability for each parametrization are within the constraints of $\Lambda_{1.4M_{\odot}} \leq 800$ and $\tilde{\Lambda} \leq 800$ imposed by the gravitational wave event GW170817[5].

It can be concluded then, that the value of $\delta = 0.05$, which models two *stiff* EoS in Fig. 1, is better than $\delta = 0.2$, which softens the EoS, to describe the studied observations. On the other hand, the values of $\gamma = 0.4$ and $\gamma = 0.6$ are equally valid and both reproduce similar results.

Acknowledgments

I would like to thank Àngels Ramos Gomez for introducing me to this fascinating research on neutron stars and guiding me during this project.

[1] J. Antoniadis et al. A Massive Pulsar in a Compact Relativistic Binary. *Science*, 340(6131), 2013.

[2] H.T. Cromartie et al. Relativistic Shapiro delay measurements of an extremely massive millisecond pulsar. *Nature Astronomy*, 4(1), 2019.

[3] M.C. Miller et al. PSR J0030+0451 Mass and Radius from NICER Data and Implications for the Properties of Neutron Star Matter. *The Astrophysical Journal*, 887(1), 2019.

[4] T.E. Riley et al. A NICER View of PSRJ0030+0451: Millisecond Pulsar Parameter Estimation. *The Astrophysical Journal*, 887(1), 2019.

[5] B.P. Abbott et al. GW170817: Observation of Gravitational Waves from a Binary Neutron Star Inspiral. *Physical Review Letters*, 119(16), 2017.

[6] B.P. Abbott et al. GW170817: Measurements of Neutron Star Radii and Equation of State. *Physical Review Letters*, 121(16), 2018.

[7] H. Heiselberg and M. Hjorth-Jensen. Phases of dense matter in neutron stars. *Physics Reports*, 328(5-6), 2000.

[8] M. Oertel et al. Equations of state for supernovae and compact stars. *Reviews of Modern Physics*, 89(1), 2017.

[9] X. Roca-Maza et al. Neutron skin thickness from the measured electric dipole polarizability in ^{68}Ni, ^{120}Sn, and ^{208}Pb. *Phys. Rev. C*, 92:064304, 2015.

[10] P.l. Danielewicz. Determination of the Equation of State of Dense Matter. *Science*, 298(5598), 2002.

[11] W.G. Lynch et al. Probing the symmetry energy with heavy ions. *Progress in Particle and Nuclear Physics*, 62(2):427–432, 2009.

[12] C. Fuchs et al. Probing the Nuclear Equation of State byK+ Production in Heavy-Ion Collisions. *Physical Review Letters*, 86(10):1974–1977, 2001.

[13] N. Hornick et al. Relativistic parameterizations of neutron matter and implications for neutron stars. *Physical Review C*, 98(6), 2018.

[14] K. Chatziioannou. Neutron-star tidal deformability and equation-of-state constraints. *General Relativity and Gravitation*, 52(11), 2020.

[15] S. Reddy and A. Watts. Neutron Stars as Multi-Messenger Laboratories for Dense Matter. Available at `https://www.youtube.com/watch?v=aVZmBCRja5k&t=495s`(2020/09/11).